Implications of JET-ILW L-H Transition Studies for ITER

J.C. Hillesheim[1], E. Delabie[2], E. R. Solano[3], C.F. Maggi[1], H. Meyer[1], E. Belonohy[4,1], I.S. Carvalho[5], E. de la Luna[3], A. Drenik[6], M. Gelfusa[7], C. Giroud[1], A.E. Hubbard[8], H.T. Kim[9], A. Huber[10], E. Lerche[11], B. Lomanowski[12], M. Mantsinen[13,14], S. Menmuir[1], I. Nunes[5], E. Peluso[7], F. Rimini[1], P.A. Schneider[6], M. Stamp[1], G. Verdoolaege[15,11] and JET Contributors *

EUROfusion Consortium JET, Culham Science Centre, Abingdon, OX14 3DB, UK
[1]CCFE, Culham Science Centre, Abingdon, Oxon OX14 3DB, United Kingdom
[2]Oak Ridge National Laboratory, Oak Ridge, Tennessee, USA
[3]Laboratorio Nacional de Fusiòn, CIEMAT, Madrid, Spain
[4]JET Exploitation Unit, Abingdon, UK
[5]Instituto de Plasmas e Fusão Nuclear, Instituto Superior Técnico, Universidade de Lisboa, Lisboa, Portugal
[6]Max-Planck-institut fur Plasmaphysik, Garching, Germany
[7]University of Rome, "Tor Vergata", Rome, Italy
[8]MIT Plasma Science and Fusion Center, Cambridge, MA, USA
[9]EUROfusion PMU, Abingdon, UK
[10]Forschungszentrum Jülich, Jülich, Germany
[11]LPP-ERM/KMS, Association EUROFUSION-Belgian State, TEC partner, Brussels, Belgium
[12]Aalto University, Aalto, Finland
[13]Barcelona Supercomputing Center, Barcelona, Spain
[14]ICREA, Barcelona, Spain
[15]Ghent University, Belgium

Corresponding Author: jon.hillesheim@ukaea.uk

Abstract:

Unraveling the conditions that permit access to H-mode continues to be an unresolved physics issue for tokamaks, and accurate extrapolations are important for planning ITER operations and DEMO design constraints. Experiments have been performed in JET, with the ITER-like W/Be wall, to increase the confidence of predictions for the L-H transition power threshold in ITER. These studies have broadly confirmed established dependencies of P_{L-H}, reduced uncertainties in extrapolations, and highlighted the largest remaining sources of uncertainty. We have also obtained unexpected results with direct relevance for lowering P_{L-H} during the non-active phase of ITER operation. A database has been

*X. Litaudon et al. Nucl. Fusion 57, 102001 (2017)

compiled of JET-ILW P_{L-H} measurements. Regression analysis of the database shows in comparison to past scaling studies and to JET-C results, P_{L-H} is lower for matched density and magnetic field; however, the exponents for density and magnetic field are larger, resulting in possibly reduced threshold at low magnetic field operation in ITER, but increased values at full field operation. The single largest uncertainty in extrapolating to ITER is the effect of the divertor configuration, a factor of two difference in JET alone. The dependence of P_{L-H} was also studied in mixed species plasmas. It was found that most of the variation in H-D mixtures was at less than 20% or more than 80% H concentration, with little variation in between. Helium-4 fuelling into H plasmas was also performed, resulting in a $\sim 25\%$ reduction of the threshold with up to about 10% He concentration. This reduction in L-H threshold in H-He mixtures may have application for the non-active phase of ITER operations.

1 Introduction

The access requirements to achieve H-mode continue to be of interest both for the physics involved, and for the design and planning constraints enforced on future experiments, including ITER and DEMO. Particularly for the early, pre-fusion power phase of ITER operation, where auxiliary heating will be installed in stages, the power required for the L-H transition will limit experiments seeking early development of ELM control techniques. DEMO designs will also be constrained by combinations of H-mode access, machine size, and power exhaust requirements. We present analysis of all available L-H transition power threshold measurements in JET with the ITER-like Be/W wall (JET-ILW) and discuss the implications of the results for future experiments.

2 JET-ILW L-H Transition Database

Figure 1 shows the result for all available JET-ILW P_{L-H} measurements, about 200 in total and expanding from previous studies [1–6], spanning a range of plasma magnetic geometries, density and toroidal magnetic field values, hydrogen isotopes, ion species mixtures, effects from impurity seeding, and differences in heating and momentum sources. The scaling prediction is taken from Ref. [7] adding a $1/m_i$ dependence [8] using measurements of the ratio between hydrogen and deuterium in the plasma such that m_{eff}=1 for pure deuterium (D) and 0.5 for hydrogen (H). The estimated core radiated power is subtracted from the thermal loss power to yield the power across the separatrix, $P_{sep} = P_L - P_{rad}$; a significant portion of the data make use of ICRH, where radiated power is correlated with the ICRH power, so the subtraction is necessary for the JET data, although this is not done in Ref. [7]. The data in Fig.1 are colored according to the location of the outer strike point, whether on the horizontal target (HT), vertical target (VT), or in the 'corner' (C/C) near the pump throat. It is notable that VT and C/C have about the same threshold, which is roughly a factor of two larger than HT. VT and C/C have very different pumping characteristics and different X-point height, which are thought to correlate with changes in P_{L-H} on other tokamaks.

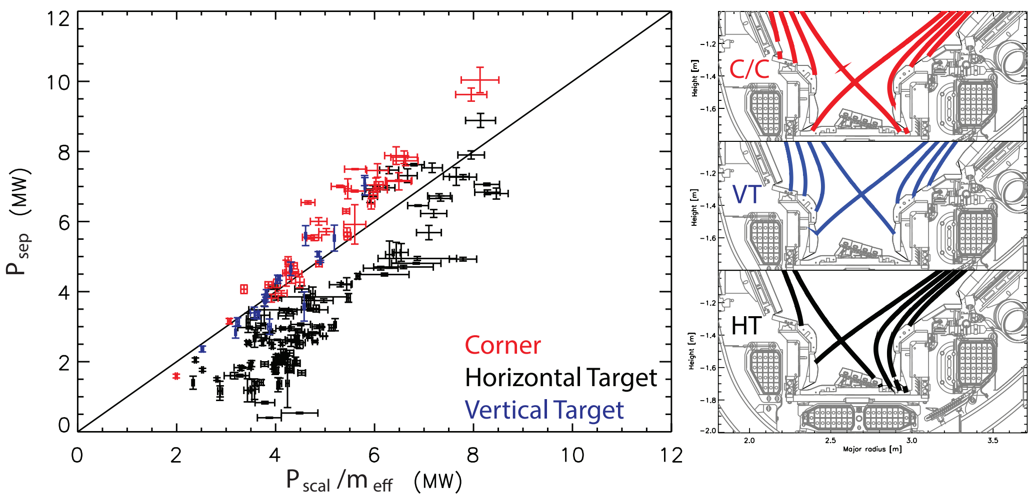

FIG. 1: Database of L-H transitions in JET-ILW, plotted against scaling law prediction [7] modified to include mass dependence and colored by divertor configuration, pictured at right.

3 Isotope and mixed ion species effects

Experiments in VT and C/C configurations were consistent with the other experiments finding P_{L-H} in H is about twice that in D [8], for the high-density branch. Variations were found for HT data, where it was possible to access the low-density branch in both H and D, and significant differences depending on heating method were identified. Fig. 2 shows the results in H, D, and 50/50 mixtures, all with the same shape, toroidal magnetic field, and plasma current. We find an isotope dependence for the value of the density at the minimum of the P_{L-H} dependence on density, due to a stronger isotope dependence in the low-density branch, also studied in AUG [9, 10]. This could affect extrapolation of the density minimum for ITER. Fig. 2 also shows that in H, P_{L-H} is much higher with NBI than ICRH, while there is little difference in D, which is similar to DIII-D results on the effect of torque [11]. Experiments in H were also performed at higher magnetic field, but were unable to access H-mode due to limited power, staying in L-mode with up to 18 MW total input power at B_t=3.2 T, even though the input power was above the scaling [7] (including $1/_{m_i}$ dependence), possibly due to the heating source effect in Fig. 2 since the majority of the heated was NBI (10 MW).

Figure 3 shows the results of scans in concentration ratio in mixed hydrogen-deuterium and hydrogen-helium plasmas, all with horizontal target magnetic configuration. The line-averaged density spans $3.1 - 3.8 \times 10^{19}$ m^{-3}, which is either in the high density branch or close to the minimum; due to the variation in density the data is normalized to the Martin scaling law[7]. Some of the variation near 50/50 H/D may be due to deviations in JET-ILW from the density dependence in the scaling law. We observe most change occurs either $H/(H + D) < 0.2$ or $H/(H + D) > 0.8$, while there is little change in between. This non-linear behavior differs from a simple $1/m_{eff}$ dependence. The strong variation at small concentration levels may indicate a role for ion-ion collisions between hydrogen and deuterium in mixed species plasmas, where the product of the isotope densities gives a parabolic dependence for the collision rate. PION ICRH simulations at the time of the transition have been performed for the H/(H+D) scan, which predict a non-monotonic dependence of the electron heat deposition, peaking at $H/(H + D) \sim 0.1 - 0.2$ and a monotonic increase in ion heating as the hydrogen fraction rises. Further transport analysis is on-going to clarify whether energy exchange can clearly dominate

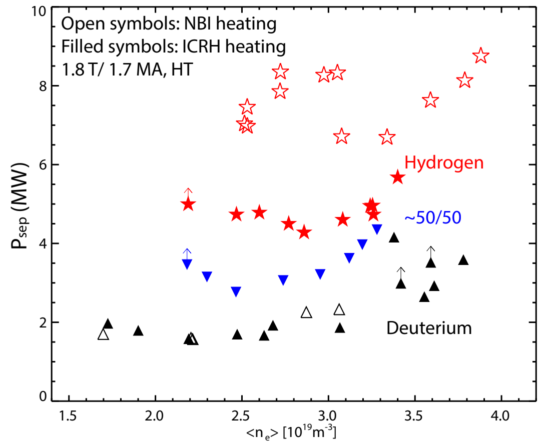

FIG. 2: L-H transition threshold in hydrogen, deuterium, and 50/50 hydrogen-deuterium mixtures. Filled symbols use ICRH heating only and open symbols use NBI heating only. Upwards arrows indicate L-mode pulses serving as lower bounds.

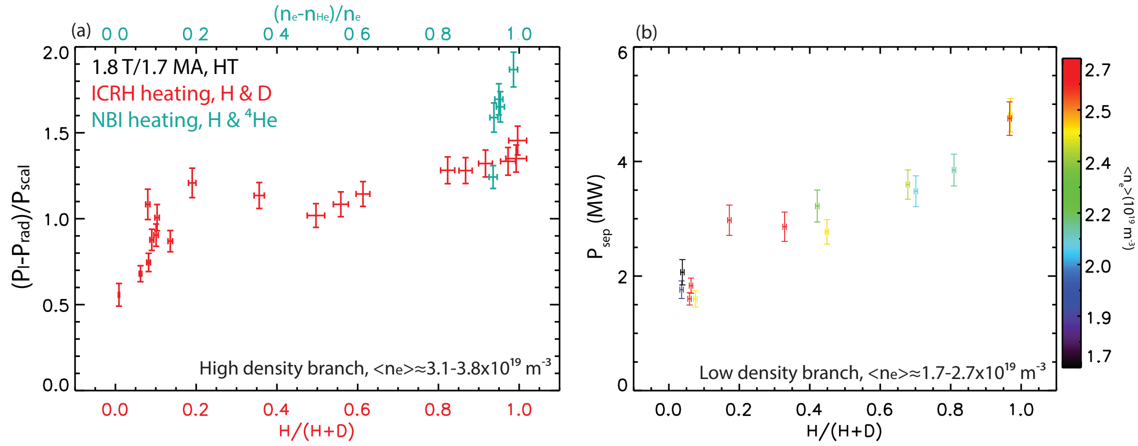

FIG. 3: (a) Dependence of L-H transition power threshold in mixed ion species plasmas, in high density branch of L-H transition. All data 1.8 T/ 1.7 MA in horizontal target divertor configuration. (b) L-H transition power threshold for hydrogen-deuterium plasmas, from the low density branch of the L-H transition. Line-averaged density for each point is indicated by color.

over the power deposition in all cases for these conditions, as is expected in the high density branch.

Figure 3(b) shows the mixed isotope scan results from the low density branch of the L-H transition. All plasmas use are 1.8 T/ 1.7 MA and use the same horizontal target shape and ICRH-only heating. The $P_{L-H,2008}$ scaling is explicitly for the high density branch only, so no normalization is applied. The color bar indicates the line-averaged density for each point. There is density variation, but the similarity of the power threshold for points at the same isotope content with different density is consistent with the observation that the density dependence, once core radiation is subtracted, for the low density branch is fairly weak. This is well illustrated by the group of points in nearly pure deuterium plasmas, with a range of densities. Since the density dependence is weak, most of the variation in Fig. 3(b) can be attributed to the isotope content of the plasma. There data are more sparse than the high density branch scan in Fig. 3(a), but there is a similar fast increase in the threshold value going from nearly pure deuterium to

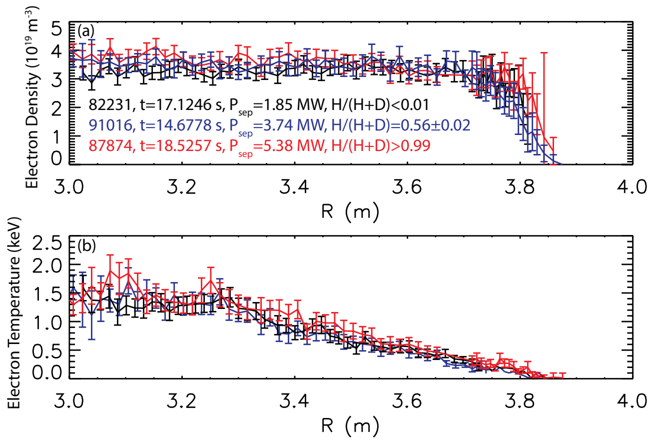

FIG. 4: (a) Electron density and (b) temperature profiles before the L-H transition for hydrogen, deuterium, and close to 50/50 mixtures H/D with ICRH heating showing the kinetic profiles prior to the transition are similar despite the large difference in heating power and power crossing the separatrix.

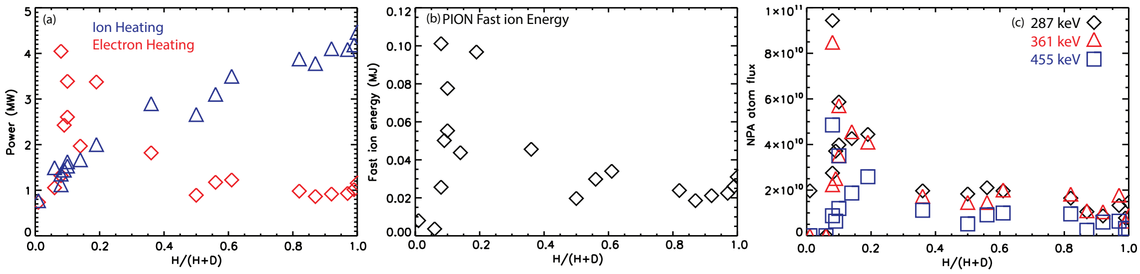

FIG. 5: (a) Heating to electrons and ions from ICRH, and (b) fast ion population energy calculated by the code PION. (c) Atom flux measured by energy channels of a neutral particle analyzer. Results are for just below the L-H transition in each plasma.

$H/(H+D) \sim 0.2$. There is a weak variation of P_{L-H} $0.2 < H/(H+D) < 0.5$. There is insufficient data to identify whether there are additional ranges with strong variation, but the threshold increases by about fifty percent from a 50/50 mixture to pure hydrogen.

Figure 4 shows electron temperature and density profiles from the Thomson scattering measurement preceding the L-H transition (5-40 ms in the different cases, all significantly less than the energy confinement time) in three cases in the ICRH-heated H/D scan shown in Fig. 3, with one hydrogen pulse, one deuterium, and one close to a 50/50 H/D mixture. Despite a large difference in the heating power and power crossing the separatrix, the profiles are essentially within measurement error of each other just prior to the transition. Due to the absence of momentum input and similar electron kinetic profiles it is reasonable to assume the edge radial electric field is also similar in all three cases – although not measured here, the edge ion temperature in similar plasmas in JET-ILW has always been found to be within uncertainties of T_e when measurements have been possible. Since the temperature and density preceding the L-H transition appears to not change, the collisionality is the same across the isotope mixture scan. This result implies that the isotopic dependence is fundamentally due to transport, with larger heating power required to attain similar profiles with the addition of hydrogen into deuterium plasmas. This is consistent with analysis of L-mode edge transport in hydrogen and deuterium plasmas, which found a large difference in edge transport depending on the hydrogenic species [12].

Due to limited data available, a conclusive understanding of the observed non-linear dependence in Fig. 3 has not been achieved. Ion temperature measurements were not available, limiting transport analysis; however, a series of simulations with TRANSP were performed varying the T_i profile to assess how much separation in temperature between ions and electrons would be possible for these plasmas. Any profiles with T_e and T_i different by 10% or more had unphysically large heat exchange compared to the input heating power, which implies $T_e \approx T_i$ in these plasmas. A sequence of PION [19] simulations of the ICRH heating to the ions and electrons were performed for the high density H/D scan (Fig. 3), shown in Fig. 5, at the time just prior to the L-H transition. The ICRH scheme was changed from N=1 minority heating at low hydrogen concentration ($\lesssim$ 5%) to N=2 heating above that, to enable good power coupling across the scan. Fig. 5(b) predicts generation of a fast ion population, depending non-monotonically on concentration, which is correlated with measured fast neutral particles by an NPA in Fig. 5(c). This also results in a non-monotonic peak in electron heating, while ion heating increases in more hydrogen-rich plasmas. Consider the points at $H/(H+D) \approx 0.2$ and 0.6; from Fig. 3 there is negligible difference in power threshold, but in Fig. 5 one is dominantly ion-heated and the other electron-heated. This along with the interpretive TRANSP results suggests that in these plasma conditions ions and electrons are sufficiently strongly coupled, that energy exchange can dominate over heat deposition in terms of the final heat flux at the edge of the plasma. Similarly, although the large increase in P_{L-H} is correlated with the increase in electron heating in Fig. 5 at low hydrogen concentration, P_{L-H} does not drop when the electron heating is reduced. These considerations imply that the non-monotonic dependence of P_{L-H} is not simply due to changes in heat deposition.

One possible hypothesis for the non-monotonic dependence of P_{L-H} would be if hydrogen-deuterium collisions are introducing an additional time scale. Ion-ion collisions depend on the product of the density of the species, which is a roughly parabolic dependence on $H/(H+D)$, such that there is rapid change in close to pure plasmas, but the collisions may quickly become much faster than other dynamical processes such that over the broad middle range in mixed plasmas, the dynamics are insensitive to the exact value. Recent work identifying rapid ion particle transport in mixed species plasmas [15–17] could also play a role in allowing the plasma to quickly re-organize its internal species concentration mixture.

4 Regression analysis of JET-ILW L-H transition data

Regression analysis of the database in Fig. 1 has been performed. In comparison to [7] and to JET-C results, P_{L-H} is lower for matched density and magnetic field as shown in [1]; however, the exponents for density and magnetic field are larger, resulting in possibly reduced threshold at low magnetic field operation in ITER, but increased values at full field operation. As highlighted by the data in Fig. 1, the single largest uncertainty in extrapolating to ITER is the effect of the divertor configuration, a factor of two difference in JET alone. This can be included in the regression by introducing an additional variable depending on the position of the outer strike point. This results in

$$P_{L-H,JET-ILW} = (0.046 \pm 0.009) B_t^{0.85\pm0.13} \langle n_e \rangle^{1.31\pm0.09} d_{sp}, \quad (1)$$

where $d_{sp} = 1$ for horizontal target pulses and $d_{sp} = 2.07 \pm 0.07$ for VT/Corner, and in comparison to [7] the surface area scaling has been assumed to be linear. It should be noted this includes data only from a single machine, and that for extrapolation to ITER, multi-machine

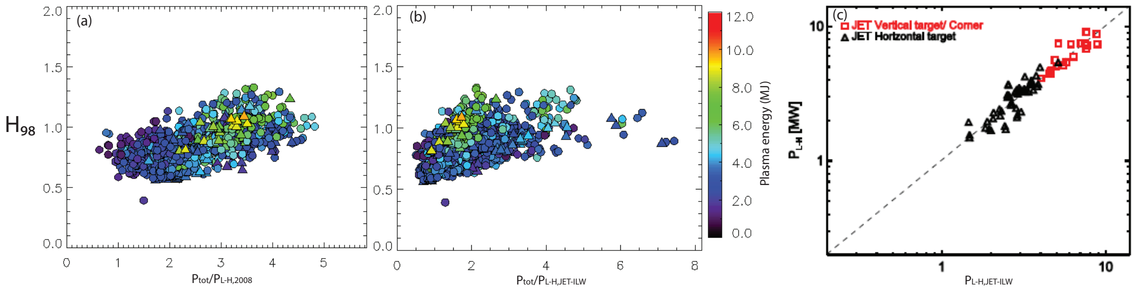

FIG. 6: Comparison of relative total input power to L-H threshold power using either (a) 2008 scaling law or (b) Eqn.1, over deuterium plasmas in JET-ILW pedestal database, showing H_{98} and stored energy. (c) Eqn.1 compared to deuterium H-mode threshold measurements.

data covering a larger domain in density and magnetic field should be used – in particular the density scaling exponent is high, which may be due to much of the data coming from close the density minimum. The leading candidate to explain the dependence on divertor configuration observed in JET-ILW is due to SOL effects and how neutral reflection pathways may have an effect on the radial electric field shear through differences in SOL and divertor temperature gradients [13, 14].

4.1 Application of JET-ILW P_{LH} scaling to pedestal database

Although Eqn. 1 should not be used for predictions of ITER due to the limited scope of the data, it does provide a useful expression for interpretation of JET-ILW results. In particular, good global confinement ($H_{98} \gtrsim 1$) has be recovered at JET-ILW at high current and stored energy, with high NBI power, usually greater than 25 MW. The heating power compared to the L-H transition power, P_{in}/P_{L-H} has sometimes been used as a proxy for predicting access to type-I ELMy H-mode conditions with good confinement. If one takes the 2008 L-H scaling then most good confinement JET-ILW results appear to be in the range $P_{in}/P_{L-H} \sim 3-4$, which is proportionally much more input power than is expected to be available in ITER. However, most of the high stored energy plasmas operate with strikes points in corner configuration ($d_{sp} = 2.06$) and relatively high density. Figure 6 compares all pulses in the JET-ILW pedestal database [18], calculating the ratio between the total input power and L-H threshold using either the 2008 scaling law or Eqn.1, over all plasmas in JET-ILW pedestal database, showing H_{98} and stored energy. Radiated power is not subtracted from the total here, which further reduces the fraction above threshold, independent of the scaling used for comparison. Fig. 6(c) shows deuterium H-mode threshold measurements compared to Eqn. 1 The group of pulses with $H_{98} \approx 1$ and stored energy approaching 10 MJ all appear at significantly lower power fraction over the threhsold when using Eqn.1.

5 Summary

The overall analysis of JET-ILW L-H transition experiments has confirmed the major trends present in multi-machine data, while also identifying several specific effects that may be important for ITER. We observe that the density minimum of the L-H threshold depends on isotope, being $\sim$ 30% higher in hydrogen than deuterium. There is a non-monotonic dependence of

P_{L-H} in mixed species plasmas, with most of the change observed in small deviations from pure plasmas. In particular we observe a significant reduction in P_{L-H} in H-^{4}He plasmas with $\sim 10\%$ ^{4}He – this could be highly relevant for pre-fusion power operation of ITER if this reduces the L-H threshold while generally maintaining the character of the pedestal and ELMs, allowing development of ELM control techniques. The largest uncertainty in extrapolating to ITER is the role of the plasma divertor configuration and divertor physics, where the position of the outer strike point can account for a factor of 2 difference in JET data alone. Regression of the JET-ILW L-H threshold data shows a stronger scaling with density and magnetic field than Ref. [7]; for updated extrapolation to ITER, a new scaling with multi-machine metal wall data should be developed and used. Using the JET-ILW scaling instead of Ref. [7] shows that many high stored energy, good confinement pulses are at significantly lower ratio of input power compared to the threshold power, which is more similar to the regime ITER is expected to operate, although the role of core radiated power should be taken into account in extrapolations.

Acknowledgments

This work has been carried out within the framework of the EUROfusion Consortium and has received funding from the Euratom research and training programme 2014-2018 under grant agreement No 633053. The views and opinions expressed herein do not necessarily reflect those of the European Commission.

References

[1] C.F. Maggi *et al.*, Nucl. Fusion **54** 023007 (2014).
[2] H. Meyer *et al.*, *Proceedings of* 41^{st} *European Physics Society Conference on Plasma Physics*, P1.013 (2014).
[3] E. Delabie *et al.*, *Proceedings of the 25th IAEA Fusion Energy Conference*, Saint Petersburg, Russia , EX/P5 (2014).
[4] E. Delabie *et al.*, *Proceedings of 42nd European Physics Society Conference on Plasma Physics*, O3.113 (2015).
[5] C.F. Maggi *et al.*, *Proceedings of* 41^{st} *European Physics Society Conference on Plasma Physics*, P1.004 (2014).
[6] J.C. Hillesheim *et al.*, Physical Review Letters **116**, 065002 (2016).
[7] Y.R. Martin *et al.*, Journal of Physics: Conference Series **123**, 012033 (2008).
[8] Righi et al., Nucl. Fusion **39**, 309 (1999).
[9] Ryter et al, Nucl. Fusion **53**, 113003 (2013).
[10] Ryter et al., Plasma Phys. Control. Fusion **58**, 014007 (2016).
[11] Gohil et al., Nucl. Fusion **50**, 064011 (2010).
[12] Maggi et al., Plasma Phys. Control. Fusion **60**, 014045 (2018)
[13] Chankin et al., Plasma Phys. Control. Fusion **59**, 045012 (2017).
[14] Moulton et al, Nuclear Fusion **58**, 096029 (2018).
[15] M. Marin et al., *Proceedings of 45th European Physics Society Conference on Plasma Physics*, (2018).
[16] C. Bourdelle et al., Nucl. Fusion **58**, 076028 (2018).
[17] M. Maslov et al., Nucl. Fusion **58**, 076022 (2018).
[18] L. Frassinetti et al., *Proceedings of 45th European Physics Society Conference on Plasma Physics*, (2018).
[19] L. G. Eriksson and T. Hellsten, Physics Scripta, Vol. 52, p. 70 (1995).